

# Synthesis and Catalytic Properties of Metal–*N*-Heterocyclic-Carbene-Decorated Covalent Organic Framework

Yue Li, Ying Dong,\* Jing-Lan Kan, Xiaowei Wu, and Yu-Bin Dong\*



Cite This: <https://dx.doi.org/10.1021/acs.orglett.0c02721>



Read Online

ACCESS |



Metrics & More

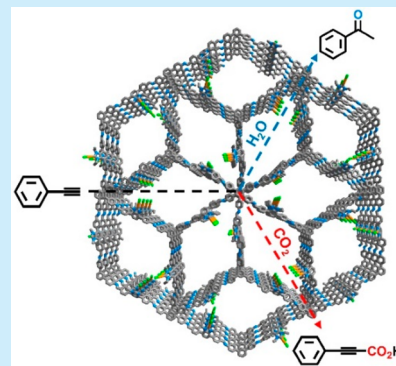


Article Recommendations



Supporting Information

**ABSTRACT:** We demonstrate herein that the *N*-heterocyclic-carbene (NHC)–metal complex (NHC–M)-involved covalent organic framework (COF) can be prepared by the direct polymerization of the NHC–M monomer with its counterpart under solvothermal conditions. The NHC–M–COF with different counterions is readily achieved via solid-state anion exchange. The obtained NHC–AuX–COF (X = Cl<sup>−</sup> and SbF<sub>6</sub><sup>−</sup>) can be a highly active reusable catalyst to separately promote the carboxylation of the terminal alkyne with CO<sub>2</sub> and alkyne hydration under mild conditions.



Since Arduengo et al. reported the first stable and isolable *N*-heterocyclic carbene (NHC),<sup>1</sup> NHC–metal (NHC–M) complexes have been recognized as an important class of organometallic catalysts.<sup>2</sup> However, the recycling and reuse of NHC–M catalysts remains challenging because the molecular NHC–M complexes are typically of single use in catalysis.<sup>3</sup> To meet the multifaceted requirements of low-cost, resource-saving, and environment-friendly synthesis, molecular NHC–M complexes are intelligently loaded on solid supports, such as metal–organic frameworks (MOFs)<sup>4</sup> and organic polymers,<sup>5</sup> by chemists to realize the catalysis in a heterogeneous way.

Since Yaghi et al. reported the first example of a covalent organic framework (COF),<sup>6</sup> COF-based chemistry has experienced rapid development.<sup>7–11</sup> It is of note that COFs possess capacious and expedite channels that can not only facilitate the transport of reactants and products but also provide efficient access to catalytic sites within the COFs. These inborn features could endow COFs with more advantages for their applications in heterogeneous catalysis.<sup>9</sup>

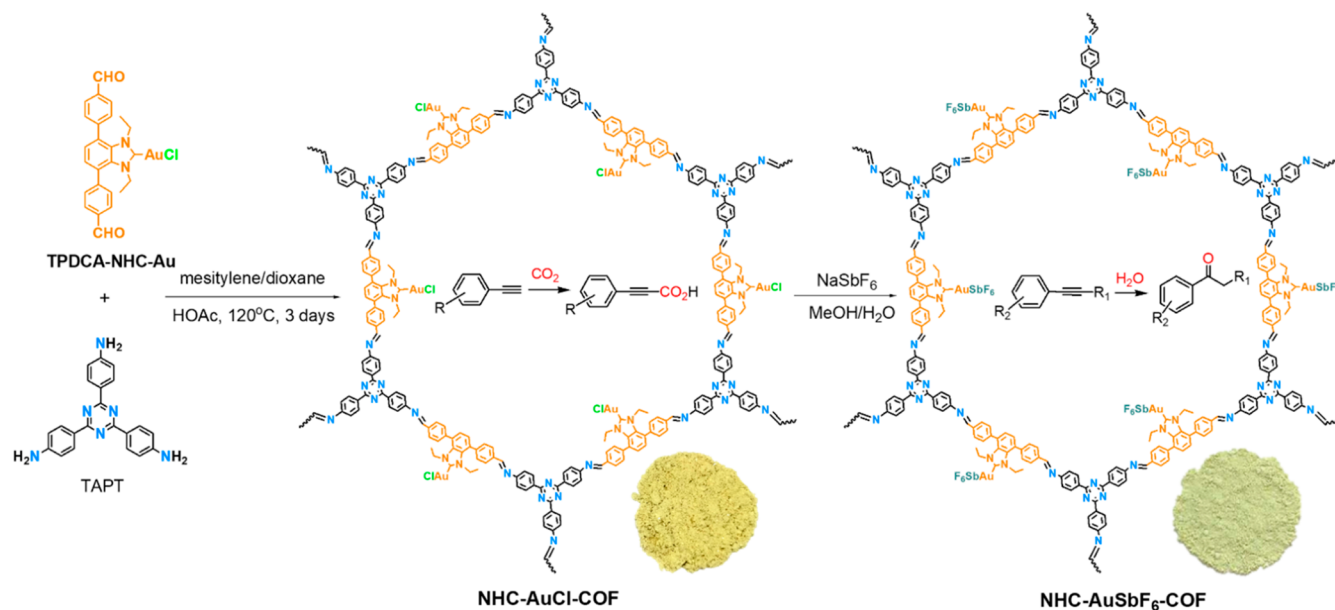
As we know, COF catalysts can be prepared by introducing the catalytic species into COFs via direct polymerization or postsynthetic modifications (PSMs).<sup>9</sup> Compared with direct polymerization, the PSM approach might sometimes result in less loading of the catalytic moieties with relatively uneven distributions because not all PSM reactions are quantitative, especially for those large-sized substrates under solid-state conditions.<sup>12</sup> We wonder if the NHC–M–COFs could be prepared by the direct polymerization of NHC–M organometallic monomers with their counterparts. In doing so, both the high catalyst loading and their uniform distribution in the COF would be realized; furthermore, the catalyst leaching

during the catalytic process could be effectively avoided. Compared with the reported organocatalysts and metal-nanoparticle-loaded COF catalysts,<sup>12</sup> the synthesis of NHC–M–COFs in this way is unprecedented thus far.

Continuing with our research on the synthesis of COFs and their catalytic applications,<sup>13</sup> we report herein, for the first time, NHC–AuCl–COF, which was generated from an NHC–AuCl-decorated 4,4′-*p*-terphenyldicarboxaldehyde monomer (TPDCA–NHC–Au) and 1,3,5-tris(4-aminophenyl)triazine (TAPT) via direct polymerization under solvothermal conditions. By anion exchange, NHC–AuSbF<sub>6</sub>–COF with different counterions was also synthesized. The obtained NHC–AuX–COF (X = Cl<sup>−</sup>, SbF<sub>6</sub><sup>−</sup>) can be a highly active heterogeneous catalyst to promote terminal alkyne carboxylation with CO<sub>2</sub> and alkyne hydration under mild conditions, respectively (Scheme 1).

The NHC–Au-decorated monomer TPDCA–NHC–Au was prepared from 4,7-dibromo-1-ethyl-1*H*-benzo[*d*]imidazole via multiple synthetic steps (Supporting Information). NHC–AuCl–COF was synthesized as yellow solids through Schiff base condensation between TPDCA–NHC–Au and TAPT under solvothermal conditions (Scheme 1, Supporting Information). IR and <sup>13</sup>C CP-MAS (Figure S1) were used to establish the connectivity of the COF, and the existence of

Received: August 14, 2020

Scheme 1. Synthesis of NHC–AuX–COF (X = Cl<sup>−</sup>, SbF<sub>6</sub><sup>−</sup>) and Its Catalytic Reactions<sup>a</sup>

<sup>a</sup>Photographs of COF samples are inserted.

TPDCA–NHC–Au and TAPT monomers was directly evidenced.

Inductively coupled plasma (ICP) analysis showed that the Au content in NHC–AuCl–COF was 23.40 wt % (calcd. 24.13 wt %). The oxidation state of Au was determined by X-ray photoelectron spectroscopy (XPS) measurement, and the binding energies for Au 4f<sub>7/2</sub> and 4f<sub>5/2</sub> were 85.38 and 88.92 eV, respectively, indicating that the Au in NHC–AuCl–COF is monovalent (Figure 1a).<sup>5b</sup> NHC–AuCl–COF is highly

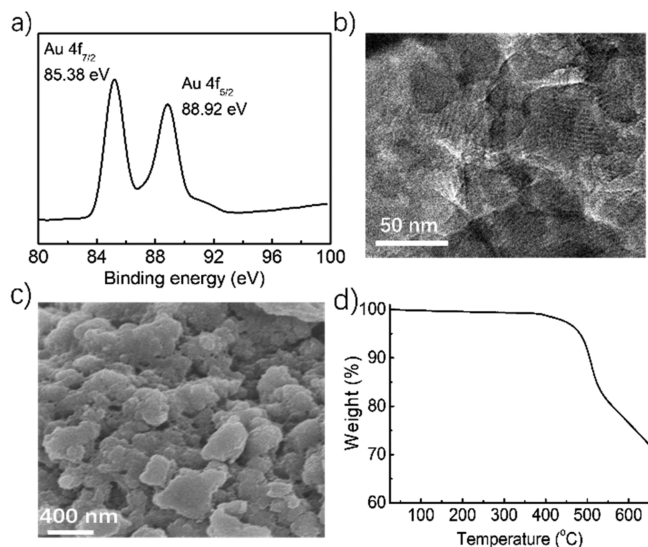
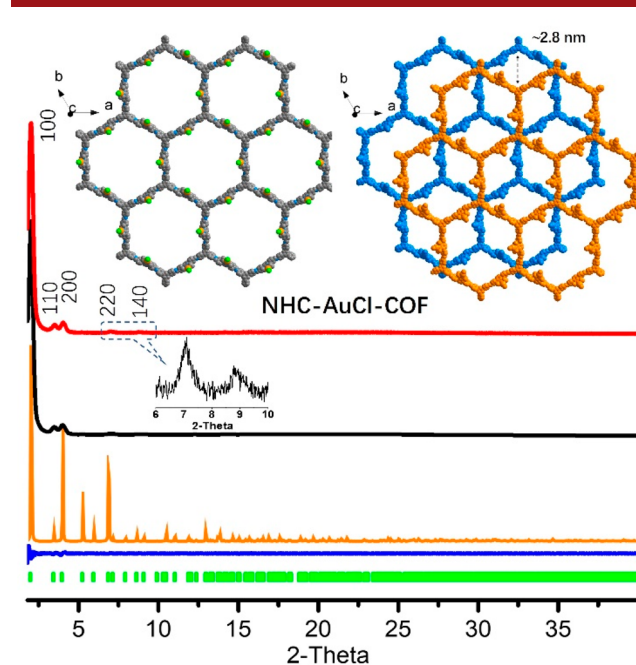


**Figure 1.** (a) XPS spectrum, (b) TEM image, (c) SEM image, and (d) TGA trace of NHC–AuCl–COF.

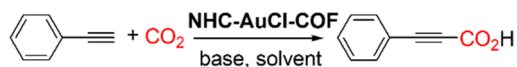
crystalline, and no Au NP was detected, which was well supported by its TEM image (Figure 1b). SEM showed that NHC–AuCl–COF features micrometer-scale lamellar morphology (Figure 1c), and the mappings of C, N, Cl, and Au indicate that their distributions are uniform (Figure S2). TGA

showed no weight loss up to ~400 °C, indicating that NHC–AuCl–COF possesses excellent thermal stability (Figure 1d).

The structural modeling of NHC–AuCl–COF was conducted with the Materials Studio (ver. 5.0) software based on the collected powder X-ray diffraction (PXRD) data (Figure 2).<sup>14</sup> Its most probable structure was a 2D staggered AB-stacking mode, and the observed diffraction peaks at 2.0, 3.4, 4.0, 6.9, and 8.9° were, respectively, assignable to the (100), (110), (200), (220), and (140) facets. The Pawley



**Figure 2.** PXRD pattern of NHC–AuCl–COF: experimental (red line) and Pawley-refined (black) profiles and the simulated pattern (orange) for the AB stacking mode. The refinement differences (blue) and the observed reflections (green) are also shown. Insets are the single and AB stacking layers in NHC–AuCl–COF.

Table 1. Optimization of the NHC–AuCl–COF-Catalyzed Carboxylation of Phenylacetylene with CO<sub>2</sub><sup>a</sup>

entry	cat. (mol % Au)	base	t (h)	solv.	T (°C)	yield (%) <sup>b</sup>
1	NHC–AuCl–COF (0.5)	Cs <sub>2</sub> CO <sub>3</sub>	16	DMSO	50	96
2	NHC–AuCl–COF (0.5)	Cs <sub>2</sub> CO <sub>3</sub>	16	DMF	50	96
3	NHC–AuCl–COF (0.5)	Cs <sub>2</sub> CO <sub>3</sub>	16	DMSO	80	96
4	NHC–AuCl–COF (0.5)	Cs <sub>2</sub> CO <sub>3</sub>	16	DMSO	20	11
5	NHC–AuCl–COF (0.5)	K <sub>2</sub> CO <sub>3</sub>	16	DMSO	50	43
6	NHC–AuCl–COF (0.3)	Cs <sub>2</sub> CO <sub>3</sub>	16	DMSO	50	78
7	NHC–AuCl–COF (1.0)	Cs <sub>2</sub> CO <sub>3</sub>	16	DMSO	50	96
8 <sup>c</sup>	NHC–AuCl–COF (0.5)	Cs <sub>2</sub> CO <sub>3</sub>	16	DMSO	50	
9		Cs <sub>2</sub> CO <sub>3</sub>	16	DMSO	50	

<sup>a</sup>CO<sub>2</sub> (1 atm), phenylacetylene (1 mmol), base (1.1 mmol), solvent (4 mL). <sup>b</sup>Isolated yields. <sup>c</sup>Without CO<sub>2</sub>. The products are determined by <sup>1</sup>H NMR, <sup>13</sup>C NMR, and MS spectra (Supporting Information).

Table 2. Optimization of the NHC–AuX–COF-Catalyzed (X = Cl<sup>−</sup>, SbF<sub>6</sub><sup>−</sup>) Model Alkyne Hydration Reaction<sup>a</sup>

entry	cat. (mol % Au)	t (h)	solv.	T (°C)	yield (%) <sup>b</sup>
1	NHC–AuCl–COF (0.5)	20	H <sub>2</sub> O	60	20
2	NHC–AuSbF <sub>6</sub> –COF (0.5)	20	H <sub>2</sub> O	60	99
3	NHC–AuSbF <sub>6</sub> –COF (0.5)	20	H <sub>2</sub> O	90	99
4	NHC–AuSbF <sub>6</sub> –COF (1.0)	20	H <sub>2</sub> O	60	99
5	NHC–AuSbF <sub>6</sub> –COF (0.5)	20	H <sub>2</sub> O	30	48
6	NHC–AuSbF <sub>6</sub> –COF (0.3)	20	H <sub>2</sub> O	60	73
7		20	H <sub>2</sub> O	60	

<sup>a</sup>Phenylacetylene (1 mmol), solvent (1 mL). <sup>b</sup>Isolated yields. The products are determined by <sup>1</sup>H NMR, <sup>13</sup>C NMR, and MS spectra (Supporting Information).

refinement (black) showed a negligible difference between the simulated (orange) and experimental PXRD pattern (red) (Figure 2). NHC–AuCl–COF was assigned to the space group *P*3 with optimized parameters of  $a = b = 52.0050 \text{ \AA}$ ,  $c = 8.0140 \text{ \AA}$ ,  $\alpha = \beta = 90^\circ$ , and  $\gamma = 120^\circ$  and residuals  $wRp = 5.88\%$  and  $Rp = 4.11\%$  (Table S1). Notably, NHC–AuCl–COF herein, with other types of possible stacking modes, gave a PXRD pattern that significantly deviated from the measured profiles (Figure S3 and Table S1).

The porosity of NHC–AuCl–COF was demonstrated by the gas adsorption–desorption measurement (Figure S4). The N<sub>2</sub> absorption amount of NHC–AuCl–COF at 77 K is 148 cm<sup>3</sup> g<sup>−1</sup>, and the corresponding surface area on the basis of the BET model is 139 m<sup>2</sup> g<sup>−1</sup>. The pore-size distribution by nonlocal density functional theory (NLDFT) analysis indicates that it possesses a narrow pore diameter distribution centered at ~2.7 nm (Figure S4).

Next, we examined the catalytic activity of NHC–AuCl–COF for the direct carboxylation of terminal alkynes with CO<sub>2</sub>, which is an economical approach for the synthesis of carboxylic acids.<sup>15</sup> On the contrary, the rational utilization of CO<sub>2</sub> is an attractive and straightforward method to reduce the greenhouse effect.<sup>16</sup>

As shown in Table 1 (entries 1–8), catalytic reactions were performed under different conditions, including different possible solvents, bases, and catalyst amounts at different temperatures. The best result was observed when the reaction was conducted in DMSO or DMF at 50 °C for 16 h (entries 1 and 2) with NHC–AuCl–COF (0.5 mol % Au equiv) and

Cs<sub>2</sub>CO<sub>3</sub> to give the carboxylation product in 96% yield (TON = 192, TOF = 12 h<sup>−1</sup>). A reaction temperature >50 °C was not conducive to increase the product yield (entry 3); meanwhile, a lower temperature (20 °C) would lead to a very low 11% yield (entry 4). In addition, when the reaction was performed in the presence of K<sub>2</sub>CO<sub>3</sub>, the product was obtained in a decreased 43% yield (entry 5). With the aid of less catalyst loading, 0.3 mol % instead of 0.5 mol %, the product was isolated in a slightly lower 78% yield (entry 6). Also, more catalyst loading could not enhance the yield (entry 7). It is of note that no desired carboxylation product was detected in the absence of CO<sub>2</sub>, indicating that the formed carboxyl group indeed came from CO<sub>2</sub> (entry 8). In addition, no product was detected without NHC–AuCl–COF (entry 9).

As a heterogeneous catalyst, NHC–AuCl–COF can be reused, and the yield of alkyne carboxylation is still up to 94%, even after five catalytic cycles, without a loss of its crystallinity or structural integrity (Figure S5). The leaching amount of Au in NHC–AuCl–COF is only ~1% (Au, 23.08 wt %), as determined by inductively coupled plasma atomic emission spectroscopy (ICP-AES), and the oxidation state of Au is intact based on the XPS (Figure S5). The postulated mechanism is believed to be the same as that of the molecular NHC–M-catalyzed alkyne carboxylation (Figure S6).<sup>16,17</sup>

The scope of NHC–AuCl–COF-catalyzed carboxylation was investigated utilizing various substrates. Besides phenylacetylene, the substituted phenylacetylenes with either electron-donating (−CH<sub>3</sub>, −C<sub>2</sub>H<sub>5</sub>, −OCH<sub>3</sub>, and −Ph) or electron-withdrawing groups (−Cl, −NO<sub>2</sub>, and −Br) at

different substituted positions furnished the excellent 95–99% yields (Table S2), implying that NHC–AuCl–COF could tolerate various functional groups under the given reaction conditions. It is of note that almost no desired products were detected from the protic functional-group-substituted (–OH) substrate or an aliphatic alkyne.

To demonstrate the generality of NHC–Au–COF in catalysis, we also evaluated its activity for alkyne hydration, which is an important reaction for the syntheses of aldehydes and ketones.<sup>18</sup> To meet the requirement of green synthesis, we performed the reaction in water. Table 2 reveals that NHC–AuCl–COF is unsatisfactory for the phenylacetylene hydration, and the acetophenone yield obtained from this model reaction is only 20% under the given conditions (0.5 mol % Au, H<sub>2</sub>O, 60 °C, 20 h). Nolan et al. reported that the molecular NHC–AuCl can effectively promote alkyne hydration but with the aid of SbF<sub>6</sub><sup>–</sup>.<sup>19</sup> Relying on these findings, together with our own results (entry 1), we then prepared NHC–AuSbF<sub>6</sub>–COF from NHC–AuCl–COF by replacing Cl<sup>–</sup> with SbF<sub>6</sub><sup>–</sup> (MeOH/H<sub>2</sub>O, 30 min, r.t., 96% yield, Supporting Information). Besides a visual color change (Scheme 1), ICP analysis showed that the Au/Sb ratio is 1:0.97 after anion exchange, implying that almost all of the Cl<sup>–</sup> in NHC–AuCl–COF has been replaced with SbF<sub>6</sub><sup>–</sup>. The Au content in NHC–AuSbF<sub>6</sub>–COF is 18.99 wt % based on the ICP-AES measurement. The PXRD pattern and SEM and TEM images after anion exchange are identical to those of NHC–AuCl–COF, suggesting that the COF structure and morphology are well maintained upon anion exchange (Figure S7). In addition, the existence of SbF<sub>6</sub><sup>–</sup> was further evidenced by the scanning electron microscopy–energy-dispersive X-ray (SEM-EDX) spectrum (Figure S7). Its corresponding surface area calculated on the basis of the BET model is 112.7 m<sup>2</sup>g<sup>–1</sup>, which is slightly less than that of NHC–AuCl–COF (Figure S8).

As expected, NHC–AuSbF<sub>6</sub>–COF exhibited excellent activity. As indicated in Table 2, the treatment of phenylacetylene with water at 60 °C afforded acetophenone in quantitative yield after 20 h (TON = 198, TOF = 9.9 h<sup>–1</sup>, entry 2) in the presence of NHC–AuSbF<sub>6</sub>–COF (0.5 mol % Au equiv). Higher temperature (90 °C, entry 3) or higher catalyst loading (1.0 mol % Au equiv, entry 4) could not enhance the hydration yield, whereas lower temperature (30 °C, entry 5) or lower catalyst loading (0.3 mol % Au equiv, entry 6) led to a modest 48 or 73% yield. Again, no product was observed without the gold catalyst (entry 7).

Again, the hot leaching test demonstrated that NHC–AuSbF<sub>6</sub>–COF was a typical heterogeneous catalyst for alkyne hydration, and the hydration yield was up to 94% yield after five catalytic cycles (Figure S9). The analysis of the NHC–AuSbF<sub>6</sub>–COF after multiple recycling by ICP-AES and XPS showed that no Au content (Au content 18.92 wt % after reuse) or valence change was detected (Figure S9). In addition, its PXRD pattern indicated that its crystallinity and structure are well maintained after multiple reuses (Figure S9). Compared with NHC–AuCl–COF (water contact angle (WCA) = 123 ± 2°), NHC–AuSbF<sub>6</sub>–COF is much more hydrophilic (WCA = 0°), so it is more suitable to promote organic reactions in aqueous phase under the applied reaction conditions (Figure S10). The mechanism of NHC–AuSbF<sub>6</sub>–COF-catalyzed alkyne hydration was supposed based on the reported molecular NHC–Au catalyst (Figure S11).<sup>20</sup>

To ascertain a scope for this COF-based catalysis, the reactivity of a series of terminal aromatic alkynes was investigated with NHC–AuSbF<sub>6</sub>–COF (Table S3). The substituted terminal aromatic alkynes with both electron-donating (–OCH<sub>3</sub>, –Ph, –C<sub>2</sub>H<sub>5</sub>) and electron-withdrawing (–Cl, –Br, –NO<sub>2</sub>) groups could be highly efficiently converted to their corresponding acetophenones (95–99% yields). However, for the internal aromatic alkyne of 4-phenyl-diphenylacetylene, the corresponding hydration product was isolated in only 50% yield, indicating that the internal alkynes are more reluctant participants than their terminal counterparts toward hydration, which is consistent with the results reported by Hayashi and Tanaka.<sup>21</sup> Additionally, 3-hydroxyphenyl acetylene and aliphatic alkyne phenyl propargyl ether could be converted into 3-hydroxyacetophenone and 1-phenoxypropan-2-one in 63 and 76% yields, respectively.

In summary, we have successfully realized the synthesis of NHC–M-involved covalent organic framework heterogeneous catalysts via a direct polymerization approach. In addition, the type of concomitant counterions in the obtained NHC–AuX–COF can be readily changed according to the requirements of different catalytic reactions. It is of note that the metal–NHC–COFs herein indicate that they showed comparable catalytic activity to that of the reported heterogeneous metal-loaded catalysts (Tables S4 and S5). We believe that our synthetic strategy provided herein is general and, moreover, significantly broadens the scope of COF catalysts.

## ■ ASSOCIATED CONTENT

### Supporting Information

The Supporting Information is available free of charge at <https://pubs.acs.org/doi/10.1021/acs.orglett.0c02721>.

Instruments and methods; synthesis and additional characterization of TPDCA–NHC–Au monomer, NHC–AuCl–COF, and NHC–AuSbF<sub>6</sub>–COF; catalytic product characterization; catalyst hot leaching and catalytic cycles; and crystallographic information for COFs (PDF)

## ■ AUTHOR INFORMATION

### Corresponding Authors

**Ying Dong** – College of Chemistry, Chemical Engineering and Materials Science, Collaborative Innovation Center of Functionalized Probes for Chemical Imaging in Universities of Shandong, Key Laboratory of Molecular and Nano Probes, Ministry of Education, Shandong Normal University, Jinan 250014, P. R. China; Email: [dongyinggreat@163.com](mailto:dongyinggreat@163.com)

**Yu-Bin Dong** – College of Chemistry, Chemical Engineering and Materials Science, Collaborative Innovation Center of Functionalized Probes for Chemical Imaging in Universities of Shandong, Key Laboratory of Molecular and Nano Probes, Ministry of Education, Shandong Normal University, Jinan 250014, P. R. China; [orcid.org/0000-0002-9698-8863](https://orcid.org/0000-0002-9698-8863); Email: [yubindong@sdsu.edu.cn](mailto:yubindong@sdsu.edu.cn)

### Authors

**Yue Li** – College of Chemistry, Chemical Engineering and Materials Science, Collaborative Innovation Center of Functionalized Probes for Chemical Imaging in Universities of Shandong, Key Laboratory of Molecular and Nano Probes, Ministry of Education, Shandong Normal University, Jinan 250014, P. R. China

Jing-Lan Kan – College of Chemistry, Chemical Engineering and Materials Science, Collaborative Innovation Center of Functionalized Probes for Chemical Imaging in Universities of Shandong, Key Laboratory of Molecular and Nano Probes, Ministry of Education, Shandong Normal University, Jinan 250014, P. R. China

Xiaowei Wu – School of Chemical Engineering, Nanjing University of Science and Technology, Nanjing, Jiangsu 210094, P. R. China

Complete contact information is available at:  
<https://pubs.acs.org/10.1021/acs.orglett.0c02721>

## Notes

The authors declare no competing financial interest.

## ACKNOWLEDGMENTS

We are grateful for financial support from the NSFC (grants 21971153, 21671122, and 21802091), Shandong Provincial Natural Science Foundation (grant ZR2018BB006), a Project of the Shandong Province Higher Educational Science and Technology Program (J18KA066), the Taishan Scholar's Construction Project, and the Changjiang Scholar project of China at SDNU.

## REFERENCES

- (1) Arduengo, A. J., III; Harlow, R. L.; Kline, M. A Stable Crystalline Carbene. *J. Am. Chem. Soc.* **1991**, *113*, 361.
- (2) (a) Hopkinson, M. N.; Richter, C.; Schedler, M.; Glorius, F. An overview of N-heterocyclic carbenes. *Nature* **2014**, *510*, 485–496. (b) Peris, E. Smart N-Heterocyclic Carbene Ligands in Catalysis. *Chem. Rev.* **2018**, *118*, 9988–10031. (c) de Fremont, P.; Marion, N.; Nolan, S. P. *Coord. Chem. Rev.* **2009**, *253*, 862–892.
- (3) Li, Y.; Dong, Y.; Wei, Y.-L.; Jv, J.-J.; Chen, Y.-Q.; Ma, J.-P.; Yao, J.-J.; Dong, Y.-B. Reusable Palladium N-Heterocyclic Tetracarbene for Aqueous Suzuki–Miyaura Cross-Coupling Reaction: Homogeneous Catalysis and Heterogeneous Recovery. *Organometallics* **2018**, *37*, 1645–1648.
- (4) (a) Oisaki, K.; Li, Q.; Furukawa, H.; Czaja, A. U.; Yaghi, O. M. A Metal-Organic Framework with Covalently Bound Organometallic Complexes. *J. Am. Chem. Soc.* **2010**, *132*, 9262–9264. (b) Dong, Y.; Li, Y.; Wei, Y.-L.; Wang, J.-C.; Ma, J.-P.; Ji, J.; Yao, B.-J.; Dong, Y.-B. A N-heterocyclic tetracarbene Pd(II) moiety containing a Pd(II)–Pb(II) bimetallic MOF for three-component cyclotrimerization via benzyne. *Chem. Commun.* **2016**, *52*, 10505–10508. (c) Wei, Y.-L.; Li, Y.; Chen, Y.-Q.; Dong, Y.; Yao, J.-J.; Han, X.-Y.; Dong, Y.-B. Pd(II)-NHDC-Functionalized UiO-67 Type MOF for Catalyzing Heck Cross-Coupling and Intermolecular Benzyne–Benzyne–Alkene Insertion Reactions. *Inorg. Chem.* **2018**, *57*, 4379–4386.
- (5) (a) Liu, C.; Kubo, K.; Wang, E.; Han, K.-S.; Yang, F.; Chen, G.; Escobedo, F. A.; Coates, G. W.; Chen, P. Single polymer growth dynamics. *Science* **2017**, *358*, 352–355. (b) Wang, W.; Zheng, A.; Zhao, P.; Xia, C.; Li, F. Au-NHC@Porous Organic Polymers: Synthetic Control and Its Catalytic Application in Alkyne Hydration Reactions. *ACS Catal.* **2014**, *4*, 321–327.
- (6) Côté, A. P.; Benin, A. I.; Ockwig, N. W.; O'Keeffe, M.; Matzger, A. J.; Yaghi, O. M. Porous, Crystalline, Covalent Organic Frameworks. *Science* **2005**, *310*, 1166–1170.
- (7) (a) Han, S. S.; Furukawa, H.; Yaghi, O. M.; Goddard, W. A. Covalent Organic Frameworks as Exceptional Hydrogen Storage Materials. *J. Am. Chem. Soc.* **2008**, *130*, 11580–11581. (b) Fan, H.; Mundstock, A.; Feldhoff, A.; Knebel, A.; Gu, J.; Meng, H.; Caro, J. Covalent Organic Framework-Covalent Organic Framework Bi-layer Membranes for Highly Selective Gas Separation. *J. Am. Chem. Soc.* **2018**, *140*, 10094–10098. (c) Wang, Z.-F.; Zhang, S.-N.; Chen, Y.; Zhang, Z.-J.; Ma, S.-Q. Covalent Organic Frameworks for Separation Applications. *Chem. Soc. Rev.* **2020**, *49*, 708–735.
- (8) (a) Lin, G.; Ding, H.; Yuan, D.; Wang, B.; Wang, C. A Pyrene-Based, Fluorescent Three-Dimensional Covalent Organic Framework. *J. Am. Chem. Soc.* **2016**, *138*, 3302–3305. (b) Hao, Q.; Zhao, C.; Sun, B.; Lu, C.; Liu, J.; Liu, M.; Wan, L.-J.; Wang, D. Confined Synthesis of Two-Dimensional Covalent Organic Framework Thin Films within Superspreading Water Layer. *J. Am. Chem. Soc.* **2018**, *140*, 12152–12158. (c) Ascherl, L.; Evans, E. W.; Hennemann, M.; Di Nuzzo, D.; Hufnagel, A. G.; Beetz, M.; Friend, R. H.; Clark, T.; Bein, T.; Auras, F. Solvatochromic Covalent Organic Frameworks. *Nat. Commun.* **2018**, *9*, 3802. (d) Wu, X.; Han, X.; Xu, Q.; Liu, Y.; Yuan, C.; Yang, S.; Liu, Y.; Jiang, J.; Cui, Y. Chiral BINOL-Based Covalent Organic Frameworks for Enantioselective Sensing. *J. Am. Chem. Soc.* **2019**, *141*, 7081–7089. (e) Liu, X.-G.; Huang, D.-L.; Lai, C.; Zeng, G.-M.; Qin, L.; Wang, H.; Yi, H.; Li, B.-S.; Liu, S.-Y.; Zhang, M.-M.; Deng, R.; Fu, Y.-K.; Li, L.; Xue, W.-J.; Chen, S. Recent Advances in Covalent Organic Frameworks (COFs) as a Smart Sensing Material. *Chem. Soc. Rev.* **2019**, *48*, 5266–5302.
- (9) (a) Ding, S. Y.; Gao, J.; Wang, Q.; Zhang, Y.; Song, W. G.; Su, C. Y.; Wang, W. Construction of Covalent Organic Framework for Catalysis: Pd/COF-LZU1 in Suzuki-Miyaura Coupling Reaction. *J. Am. Chem. Soc.* **2011**, *133*, 19816–19822. (b) Vyas, V. S.; Haase, F.; Stegbauer, L.; Savasci, G.; Podjaski, F.; Ochsenfeld, C.; Lotsch, B. V. A Tunable Azine Covalent Organic Framework Platform for Visible Light-Induced Hydrogen Generation. *Nat. Commun.* **2015**, *6*, 8508. (c) Lin, S.; Diercks, C. S.; Zhang, Y.-B.; Kornienko, N.; Nichols, E. M.; Zhao, Y.; Paris, A. R.; Kim, D.; Yang, P.; Yaghi, O. M.; Chang, C. J. Covalent Organic Frameworks Comprising Cobalt Porphyrins for Catalytic CO<sub>2</sub> Reduction in Water. *Science* **2015**, *349*, 1208–1213. (d) Sun, Q.; Aguila, B.; Perman, J.; Nguyen, N.; Ma, S. Q. Flexibility Matters: Cooperative Active Sites in Covalent Organic Framework and Threaded Ionic Polymer. *J. Am. Chem. Soc.* **2016**, *138*, 15790–1596. (e) Li, H.; Pan, Q.; Ma, Y.; Guan, X.; Xue, M.; Fang, Q.; Yan, Y.; Valtchev, V.; Qiu, S. Three-Dimensional Covalent Organic Frameworks with Dual Linkages for Bifunctional Cascade Catalysis. *J. Am. Chem. Soc.* **2016**, *138*, 14783–14788. (f) Lu, S.; Hu, Y.; Wan, S.; McCaffrey, R.; Jin, Y.; Gu, H.; Zhang, W. Synthesis of Ultrafine and Highly Dispersed Metal Nanoparticles Confined in a Thioether-Containing Covalent Organic Framework and Their Catalytic Applications. *J. Am. Chem. Soc.* **2017**, *139*, 17082–17088. (g) Pachfule, P.; Acharjya, A.; Roeser, J.; Langenhahn, T.; Schwarze, M.; Schomäcker, R.; Thomas, A.; Schmidt, J. Diacetylene Functionalized Covalent Organic Framework (COF) for Photocatalytic Hydrogen Generation. *J. Am. Chem. Soc.* **2018**, *140*, 1423–1427. (h) Yang, J.; Wu, Y.; Wu, X.; Liu, W.; Wang, Y.; Wang, J. An N-Heterocyclic Carbene-functionalized Covalent Organic Framework with Atomically Dispersed Palladium for Coupling Reactions under Mild Conditions. *Green Chem.* **2019**, *21*, 5267–5273. (i) Wang, Y.; Liu, H.; Pan, Q.; Wu, C.; Hao, W.; Xu, J.; Chen, R.; Liu, J.; Li, Z.; Zhao, Y. Construction of Fully Conjugated Covalent Organic Frameworks via Facile Linkage Conversion for Efficient Photoenzymatic Catalysis. *J. Am. Chem. Soc.* **2020**, *142*, 5958–5963. (j) Guo, J.; Jiang, D.-L. Covalent Organic Frameworks for Heterogeneous Catalysis: Principle, Current Status, and Challenges. *ACS Cent. Sci.* **2020**, *6*, 869–879.
- (10) (a) Vyas, V. S.; Vishwakarma, M.; Moudrakovski, I.; Haase, F.; Savasci, G.; Ochsenfeld, C.; Spatz, J. P.; Lotsch, B. V. Exploiting Noncovalent Interactions in an Imine-Based Covalent Organic Framework for Quercetin Delivery. *Adv. Mater.* **2016**, *28*, 8749–8754. (b) Zhang, G.; Li, X.; Liao, Q.; Liu, Y.; Xi, K.; Huang, W.; Jia, X. Water-dispersible PEG-curcumin/amine-functionalized covalent organic framework nanocomposites as smart carriers for in vivo drug delivery. *Nat. Commun.* **2018**, *9*, 2785. (c) Guan, Q.; Fu, D.-D.; Li, Y.-A.; Kong, X.-M.; Wei, Z.-Y.; Li, W.-Y.; Zhang, S.-J.; Dong, Y.-B. BODIPY-Decorated Nanoscale Covalent Organic Frameworks for Photodynamic Therapy. *iScience* **2019**, *14*, 180–198. (d) Guan, Q.; Zhou, L.-L.; Li, Y.-A.; Li, W.-Y.; Wang, S.; Song, C.; Dong, Y.-B. Nanoscale Covalent Organic Framework for Combinatorial Antitumor Photodynamic and Photothermal Therapy. *ACS Nano* **2019**, *13*, 13304–13316. (e) Guan, Q.; Zhou, L.-L.; Li, W.-Y.; Li, Y.-A.;

- Dong, Y.-B. Covalent Organic Frameworks (COFs) for Cancer Therapeutics. *Chem. - Eur. J.* **2020**, *26*, 5583–5591 and references therein. (f) Guan, Q.; Zhou, L.-L.; Lv, F.-H.; Li, W.-Y.; Li, Y.-A.; Dong, Y.-B. Nanoscale covalent organic frameworks as theranostic platforms for oncotherapy: synthesis, functionalization, and applications. *Angew. Chem., Int. Ed.* **2020**, DOI: [10.1002/anie.202008055](https://doi.org/10.1002/anie.202008055). (g) Guan, Q.; Wang, G.-B.; Zhou, L.-L.; Li, W.-Y.; Dong, Y.-B. *Nanoscale Adv.* **2020**, DOI: [10.1039/D0NA00537A](https://doi.org/10.1039/D0NA00537A), and references therein. (h) Bhunia, S.; Deo, K. A.; Gaharwar, A. K. Gaharwar, 2D Covalent Organic Frameworks for Biomedical Applications. *Adv. Funct. Mater.* **2020**, *30*, 2002046.
- (11) (a) Wan, S.; Guo, J.; Kim, J.; Ihee, H.; Jiang, D. A Belt-Shaped, Blue Luminescent, and Semiconducting Covalent Organic Framework. *Angew. Chem., Int. Ed.* **2008**, *47*, 8826–8830. (b) Bertrand, G. H. V.; Michaelis, V. K.; Ong, T. C.; Griffin, R. G.; Dinca, M. Thiophene-Based Covalent Organic Frameworks. *Proc. Natl. Acad. Sci. U. S. A.* **2013**, *110*, 4923–4928. (c) Dogru, M.; Handloser, M.; Auras, F.; Kunz, T.; Medina, D.; Hartschuh, A.; Knochel, P.; Bein, T. A Photoconductive Thienothio-phene-Based Covalent Organic Framework Showing Charge Transfer Towards Included Fullerene. *Angew. Chem., Int. Ed.* **2013**, *52*, 2920–2996. (d) Du, Y.; Yang, H.; Whiteley, J. M.; Wan, S.; Jin, Y.; Lee, S. H.; Zhang, W. Ionic Covalent Organic Frameworks with Spiroborate Linkage. *Angew. Chem., Int. Ed.* **2016**, *55*, 1737–1741. (e) Li, H.; Chang, J.; Li, S.; Guan, X.; Li, D.; Li, C.; Tang, L.; Xue, M.; Yan, Y.; Valtchev, V.; Qiu, S.; Fang, Q. Three-Dimensional Tetrathiafulvalene-Based Covalent Organic Frameworks for Tunable Electrical Conductivity. *J. Am. Chem. Soc.* **2019**, *141*, 13324–13329. (f) Yuan, S.; Li, X.; Zhu, J.; Zhang, G.; Van Puyvelde, P.; Van der Bruggen, B. Peter Van Puyvelde, Bart Van der Bruggen. Covalent Organic Frameworks for Membrane Separation. *Chem. Soc. Rev.* **2019**, *48*, 2665–2681.
- (12) Ma, H.-C.; Zou, J.; Li, X.-T.; Chen, G.-J.; Dong, Y.-B. Homochiral Covalent Organic Frameworks for Asymmetric Catalysis. *Chem. - Eur. J.* **2020**, DOI: [10.1002/chem.202001006](https://doi.org/10.1002/chem.202001006), and references therein.
- (13) (a) Ma, H.-C.; Kan, J.-L.; Chen, G.-J.; Chen, C.-X.; Dong, Y.-B. Pd NPs-Loaded Homochiral Covalent Organic Framework for Heterogeneous Asymmetric Catalysis. *Chem. Mater.* **2017**, *29*, 6518–6524. (b) Ma, H.-C.; Zhao, C.-C.; Chen, G.-J.; Dong, Y.-B. Photothermal conversion triggered thermal asymmetric catalysis within metal nanoparticles loaded homochiral covalent organic framework. *Nat. Commun.* **2019**, *10*, 3368. (c) Li, X.-T.; Zou, J.; Wang, T.-H.; Ma, H.-C.; Chen, G.-J.; Dong, Y.-B. Construction of Covalent Organic Frameworks via Three-Component One-Pot Strecker and Povarov Reactions. *J. Am. Chem. Soc.* **2020**, *142*, 6521–6526. (d) Ma, H.-C.; Chen, G.-J.; Huang, F.; Dong, Y.-B. Homochiral Covalent Organic Framework for Catalytic Asymmetric Synthesis of a Drug Intermediate. *J. Am. Chem. Soc.* **2020**, *142*, 12574–12578.
- (14) *Materials Studio, Release Notes*; Accelrys Software, 2018.
- (15) (a) Gooßen, L. J.; Rodriguez, N.; Manjolinho, F.; Lange, P. P. Synthesis of Propiolic Acids via Copper-Catalyzed Insertion of Carbon Dioxide into the C-H Bond of Terminal Alkynes. *Adv. Synth. Catal.* **2010**, *352*, 2913–2917. (b) Yu, D.; Zhang, Y. Copper- and copper-N-heterocyclic carbene-catalyzed C-H activating carboxylation of terminal alkynes with CO<sub>2</sub> at ambient conditions. *Proc. Natl. Acad. Sci. U. S. A.* **2010**, *107*, 20184–20189. (c) Zhang, X.; Zhang, W.-Z.; Ren, X.; Zhang, L.-L.; Lu, X.-B. Ligand-Free Ag(I)-Catalyzed Carboxylation of Terminal Alkynes with CO<sub>2</sub>. *Org. Lett.* **2011**, *13*, 2402–2405.
- (16) Bui, M.; Adjiman, C. S.; Bardow, A.; Anthony, E. J.; Boston, A.; Brown, S.; Fennell, P. S.; Fuss, S.; Galindo, A.; Hackett, L. A.; Hallett, J. P.; Herzog, H. J.; Jackson, G.; Kemper, J.; Krevor, S.; Maitland, G. C.; Matuszewski, M.; Metcalfe, I. S.; Petit, C.; Puxty, G.; Reimer, J.; Reiner, D. M.; Rubin, E. S.; Scott, S. A.; Shah, N.; Smit, B.; Trusler, J. P. M.; Webley, P.; Wilcox, J.; Mac Dowell, N. Carbon capture and storage (CCS): the way forward. *Energy Environ. Sci.* **2018**, *11*, 1062–1176.
- (17) Manjolinho, F.; Arndt, M.; Gooßen, K.; Gooßen, L. J. Catalytic C–H Carboxylation of Terminal Alkynes with Carbon Dioxide. *ACS Catal.* **2012**, *2*, 2014–2021.
- (18) Steinborn, D. In *Fundamentals of Organometallic Catalysis*, 1st ed.; Wiley-VCH: Weinheim, Germany, 2011.
- (19) Marion, N.; Ramón, R. S.; Nolan, S. P. [(NHC)AuI]-Catalyzed Acid-Free Alkyne Hydration at Part-per-Million Catalyst Loadings. *J. Am. Chem. Soc.* **2009**, *131*, 448–449.
- (20) (a) Ibrahim, H.; de Frémont, P.; Braunstein, P.; Théry, V.; Nauton, L.; Cisnetti, F.; Gautier, A. Water-Soluble Gold-N-Heterocyclic Carbene Complexes for the Catalytic Homogeneous Acid- and Silver-Free Hydration of Hydrophilic Alkynes. *Adv. Synth. Catal.* **2015**, *357*, 3893–3900. (b) Casado, R.; Contel, M.; Laguna, M.; Romero, P.; Sanz, S. Organometallic Gold(III) Compounds as Catalysts for the Addition of Water and Methanol to Terminal Alkynes. *J. Am. Chem. Soc.* **2003**, *125*, 11925–11935.
- (21) (a) Mizushima, E.; Sato, K.; Hayashi, T.; Tanaka, M. Highly Efficient AuI-Catalyzed Hydration of Alkynes. *Angew. Chem., Int. Ed.* **2002**, *41*, 4563–4565. (b) Mizushima, E.; Cui, D.-M.; Nath, D. C. D.; Hayashi, T.; Tanaka, M. Au(I)-Catalyzed Hydration of Alkynes: 2,8-Nonanedione. *Org. Synth.* **2006**, *83*, 55–60.